JOURNAL OF CATALYSIS **80**, 328–339 (1983)

Dependence of the Kinetics of the Low-Temperature Water–Gas Shift Reaction on the Catalyst Oxygen Activity as Investigated by Wavefront Analysis

E. FIOLITAKIS AND H. HOFMANN

Institut für Technische Chemie I der Universität Erlangen, Egerlandstrasse 3, D-8520 Erlangen, West Germany

Received August 21, 1980; revised August 21, 1981

The systematic investigation by means of wavefront analysis of the dependence of the microkinetics of the water–gas shift reaction on the oxidation state of a CuO/ZnO industrial catalyst is reported. The catalyst was pretreated for a long period of time in a mixture of H_2O, H_2, and N_2 at definite $\psi = p_{H_2O}/p_{H_2}$ ratios, from $\psi = 0.1$ to $\psi = 10.0$ and at 230°C. The fitting procedure at different ψ levels suggested a three-path reaction model consisting of two formal Eley–Rideal-type mechanisms which are relevant for the microkinetic shift conversion through adsorption intermediates of CO and H_2O, and a redox mechanism which regulates the oxygen activity on the catalyst surface and accounts for the interaction catalyst/reaction medium. In this investigation, an Elovich-type rate dependence of the redox mechanism has been suggested.

INTRODUCTION

Heterogeneous catalytic conversions proceed by the participation of some surface intermediates on the catalyst surface. Contrary to widespread opinion, solid catalysts do not remain invariant after their exposure to the reaction medium. Their chemical composition, surface structure, and/or other catalytic properties change in dependence on the composition of the reaction mixture and temperature. Thus, each change in the ambient fluid causes a relaxation of the catalyst itself, the corresponding relaxation times being as a rule very large. However, at elevated (technical) temperatures this process is fast enough and is well observable under transient conditions. This kind of interaction between solid catalyst and reaction medium has been recognized by Wagner and his research group (*1*) and by Soviet scientists such as Temkin (*2*) and Boreskov (*3*).

We report here a systematic investigation to estimate quantitatively the change in the overall activity as well as the shift in the mechanistic scheme in dependence on the oxidation state of the catalyst.

As stated correctly by Boreskov (*3*), a consequence of the interaction between solid catalyst and ambient fluid is that the change in the catalytic properties causes a change in the reaction rate. A genuine kinetic investigation demands therefore to find out the whole rate functional which describes the influence of the catalyst on the reaction medium (i.e., corresponds to the stoichiometry of the chemical conversion) and at the same time describes the influence of the reaction medium on the catalyst. Unfortunately, this functional is of a rather complex nature so that special techniques (such as the one discussed here) should be applied in order to separate the two kinds of dependences of the reaction rate.

Following Temkin (*2*), we define as *intrinsic* or *microkinetic relaxations* the relaxation processes of the conversion on the catalyst surface through sorption intermediates (i.e., chemisorption, surface reaction, desorption), and as *extrinsic* or *macrokinetic relaxations* the relaxation

0021-9517/83 $3.00

processes of the influence of reaction mixture on the catalyst (i.e., change in the catalytic properties).

PRINCIPLES OF WAVEFRONT ANALYSIS

The wavefront analysis of reaction kinetics is a special transient technique for kinetic investigations in continuous flow, disturbed heterogeneous catalytic systems under technical operating conditions. It has been introduced in Ref. (*4*) and presented in Ref. (*5*) in a more detailed and improved form, together with several applications. A complete mathematical presentation, further theoretical advances and additional applications of this technique in connection with complex catalytic processes are contained in a comprehensive treatise by one of us (*6*).

The new technique is an enlargement of known relaxation methods in the sense that it considers in addition to the transition of the disturbed system from the initial to the end steady state, the relaxation in space of the propagating primary disturbance (for clear definition of the front, a step disturbance is used). Actually, the wavefront analysis is limited to the relaxation processes at the wavefront and the propagation line of the disturbance in the space/time coordinate plane. It supplies an additional degree of freedom compared to a stationary analysis.

We define as *space relaxation* the amplitude change of the propagating disturbance, as *time relaxation* the rest of the transient response after passage of the wavefront, i.e., the transient originated by the propagated primary disturbance. The elements of the analysis are:

- The propagation speed of the disturbance, controlled by capacitive effects in the phases (i.e., chromatographic effects),
- The space relaxation of the disturbance, representing a measure of the initial rate (i.e., initial relaxation),
- The time gradient of the time relaxation at the front of the disturbance, representing a measure of the initial rate acceleration (*6*) (i.e., acceleration of the initial relaxation).

In this way, a splitting of the information content of the transient response in pure accumulative and kinetic parts is achieved (see Table 1) and in addition initial rate and initial acceleration are directly measurable in dependence on well-defined initial states of temperature and catalyst activities. For practical applications, it is important that the time relaxation is slower than the change on what is practically defined as a "wavefront," which means slower than the space relaxation of the front of the disturbance. Short-range chromatographic effects are not kinetically relevant as long as their action is much shorter than the time constant of the time relaxation (on space relaxation basis, see (*6*)).

NOMENCLATURE

c	gas phase concentration (kmol/m^3 gas)
$k'_{1,2,3,4}$	effective rate constants (s^{-1}), see text
K_p	thermodynamic equilibrium constant of the water–gas shift reaction
$m_{1,2}$	eigenvalues for the space relaxation (s^{-1})
p_i	partial pressure
r_i	reaction rate
t	time
t'	time measured on the propagating wavefront
T	temperature (K)

Greek Symbols

α_0	propagation line of the wavefront
Δc	concentration disturbance
$\Delta \dot{c}$	time gradient of the time relaxation
θ	oxygen activity of the catalyst surface (kg atom oxygen/m^3 catalyst)
τ_0	hydrodynamic time constant = residence time of the wavefront
ζ	equilibrium ratio p_{CO_2}/p_{CO}
ψ	equilibrium ratio p_{H_2O}/p_{H_2}

TABLE 1

Differences between Wavefront Analysis and Conventional Transient Response Techniques

Elements of transient response	Applicability	
	Wavefront analysis (Only distributed systems)	Conventional transient response techniques (Distributed and concentrated systems)
Propagation speed	Reflects the ratio of the corresponding total capacitance to the capacitance of the movable phase (convective accumulative effects)	Not available
Time relaxation	Transient response after passage of the wavefront	The whole transient response containing information about convective accumulative effects, kinetic effects corresponding to the initial steady state and to the relaxation of the whole system
Space relaxation	Amplitude change along the propagation line caused by kinetic effects corresponding to the initial steady state	Not separated

MATHEMATICAL EQUATIONS

The following two equations are important for the application of wavefront analysis to the present investigation (*5–7*).

Amplitude change of the propagating concentration step disturbance, i.e., relaxation in space,

$$(\Delta c)_{\alpha_0} = \int_0^{\tau_0} r(c_{\alpha_0}, \theta_s, T_s)\, dt', \qquad (1)$$

where t' is the time measured by an observer on the wavefront; $t' = 0$ is at the inlet of the system. Equation (1) means that the step disturbance Δc in the present investigation is meeting on the propagation line α_0 only with stationary states of temperature T_s and of catalyst (oxygen) activity θ_s. A necessary condition for exact measuring of the disturbance front is that the rate acceleration remains bounded. The time gradient of the time relaxation $\Delta\dot{c}$, which is a measure of this acceleration, obeys (*6, 7*)

$$\frac{d\Delta\dot{c}}{dt'} = \left(\frac{\partial r}{\partial c}\right)_{\alpha_0} \cdot \Delta\dot{c} + \left(\frac{\partial r}{\partial \theta}\cdot\frac{\partial \theta}{\partial t} + \frac{\partial r}{\partial T}\cdot\frac{\partial T}{\partial t}\right)_{\alpha_0}. \qquad (2)$$

Equation (2) is obtained by means of perturbation analysis at the wavefront, i.e., developing in series, Δc and r about α_0, inserting in the differential form of Eq. (1) and comparing coefficients; for more details see Refs. (*6, 7*). Its solution gives

$$\Delta\dot{c} = \left(\frac{\partial \Delta c}{\partial t}\right)_{\alpha_{0+}} = \exp\left(\int_0^{\tau_0}\left(\frac{\partial r}{\partial c}\right)_{\alpha_0} dt'\right) \cdot \int_0^{\tau_0} \exp\left(-\int_0^{t'}\left(\frac{\partial r}{\partial c}\right)_{\alpha_0} dt'\right) \cdot \left(\frac{\partial r}{\partial \theta}\cdot\frac{\partial \theta}{\partial t} + \frac{\partial r}{\partial T}\cdot\frac{\partial T}{\partial t}\right)_{\alpha_0} dt'. \qquad (3)$$

We should point out that the quantities with the suffix α_0 are only functions of the time t'; here the acceleration $\Delta\dot{c}$ has its cause in the surface effects and in thermal effects. This equation remains valid as long as the quantities in parenthesis remain simple functions of the rate r (c_{α_0}, T_s, θ_s), i.e., the partial derivatives $(\partial\theta/\partial t)_{\alpha_0}$ and $(\partial T/\partial t)_{\alpha_0}$ remain bounded.

SUMMARY OF PREVIOUS EXPERIMENTAL RESULTS AND CONCLUSIONS

The experimental setup and preliminary investigations are described elsewhere (*5, 6, 7, 8, 9*). For the water–gas shift reaction it was shown that:

(a) For a catalyst at high oxidation level at the wavefront the CO_2 production is faster than the H_2 production. A redox mechanism, which is probably responsible for the faster CO_2 production, regulates the oxygen potential over the catalyst surface and is inhibited by H_2O.

(b) For a catalyst at low oxidation level, e.g., at a state established by a long pretreatment in a CO/N_2 mixture, one obtains at the wavefront H_2 and CO_2 in the ratio 2 : 1. This is an indication that at the beginning of the reoxidation the redox reaction proceeds equally as fast as the shift reaction, i.e., the limiting step in the shift reaction is the reoxidation of the catalyst. In other words, the shift conversion is possible only after certain oxide forms have been built up on the catalyst surface. This deviation from the stoichiometry declines slowly with a time constant of about 10 min.

(c) The participation of sorption intermediates in the shift reaction could be established, where the relevant adsorption/desorption steps, i.e., CO adsorption, H_2O adsorption, CO_2 desorption, H_2 desorption under the selected experimental conditions are not kinetically controlled, as suggested by the form of the transients (*6, 10*). Further more, the adsorption/desorption characteristics seem to depend on the oxidation state and temperature of the catalyst (*6*). Thus, for example at high oxidation levels of the catalyst, H_2O adsorption proceeds by two mechanisms, one of which is probably physisorption, the other one chemisorption (*8*). At low oxidation states, the concentration of chemisorbed H_2O is higher than that at higher oxidation states but it does not participate in the shift reaction (*6, 9*), suggesting that the H_2O chemisorption sites at low oxidation level are different from those ones at higher or intermediary oxidation levels. In addition, H_2O can be removed after stripping with N_2 (*9*), i.e., H_2O is reversibly adsorbed. On the contrary, chemisorbed CO on the catalyst at low oxidation state cannot be stripped off by N_2 (*9*).

Therefore, it seems plausible that the microkinetic conversion of the reactants on the catalyst surface proceeds by participation of sorption intermediates, following a reaction mechanism of Langmuir or of Eley–Rideal type. Beyond that a redox mechanism participates, regulating the oxygen activity of the catalyst surface, whereas this change in the oxygen activity is very slow. Whether the redox mechanism is also relevant for the stationary shift conversion is an open question. However, as preliminary experiments have shown, the overall catalyst activity depends significantly on the oxidation level of the catalyst, i.e., *the slow redox reaction controls the stationary catalyst overall activity.* It therefore seemed important to investigate in detail the relationship between catalyst activity and oxidation level of the catalyst.

EXPERIMENTAL

In this investigation the catalyst of type Girdler/Südchemie G66B (with CuO/ZnO as main components) has been pretreated for several hours, until equilibrium has been established, in a mixture of $H_2O/H_2/N_2$ (technical) at defined levels of the ratio $\psi = p_{H_2O}/p_{H_2}$ over two decades, i.e., from $\psi = 0.10$ to $\psi = 10.0$. The so-pretreated catalyst has been tested thereafter by a mixture of $CO/H_2O/N_2$, the amplitude of the CO- and H_2O-concentration step having been varied between 0.06 and 0.33 bar and 0.25 and 0.67 bar, respectively, by sudden exchange of the pretreatment mixture with the test mixture. The experiments have been performed at the 230°C level at a constant flow velocity of 0.11 m^3N/h; the pretreatment phase was about 30 min, the testing phase about 3 to 5 min.

RESULTS

In order to demonstrate the application of the new technique, in Fig. 1 are depicted typical transients from a similar investigation (*11*) at a higher temperature and at a lower oxidation state of the catalyst (i.e., 280°C and $\psi = 0.01$), in order to obtain stronger effects of the catalyst reoxidation process. Here the pretreatment mixture consists of H_2 (0.50 bar), H_2O (0.005 bar), N_2 (0.495 bar). The test mixture consists of CO (0.15 bar), H_2O (0.25 bar), N_2 (0.60 bar). The testing has been performed by sudden exchange of the pretreatment mixture with the test mixture.

The wavefront amplitudes which correspond to the space relaxation of the used concentration step disturbance, are measured at the indicated time point, i.e., immediately after the short-range chromatographic effects have been finished. For instance, here the relevant chromatographic effects have their cause in the fact that CO sweeps adsorbed H_2 from the surface; this process, however, proceeds fast enough and is not kinetically controlled, generating therefore the observed equilibrium chromatographic effects.

A further inspection of the transient responses has established the following facts, in agreement with the above reported qualitative analysis: As the catalyst has been pretreated until a low oxidation state has been reached, during testing the H_2 amplitude is also here twice the CO_2 amplitude. The time relaxations show no evidence of significant adsorption/desorption effects, because the sum of H_2, H_2O as well as of CO, CO_2 transients equals the feed concentrations in the testing mixture. This means that in the time-relaxation region H_2O is

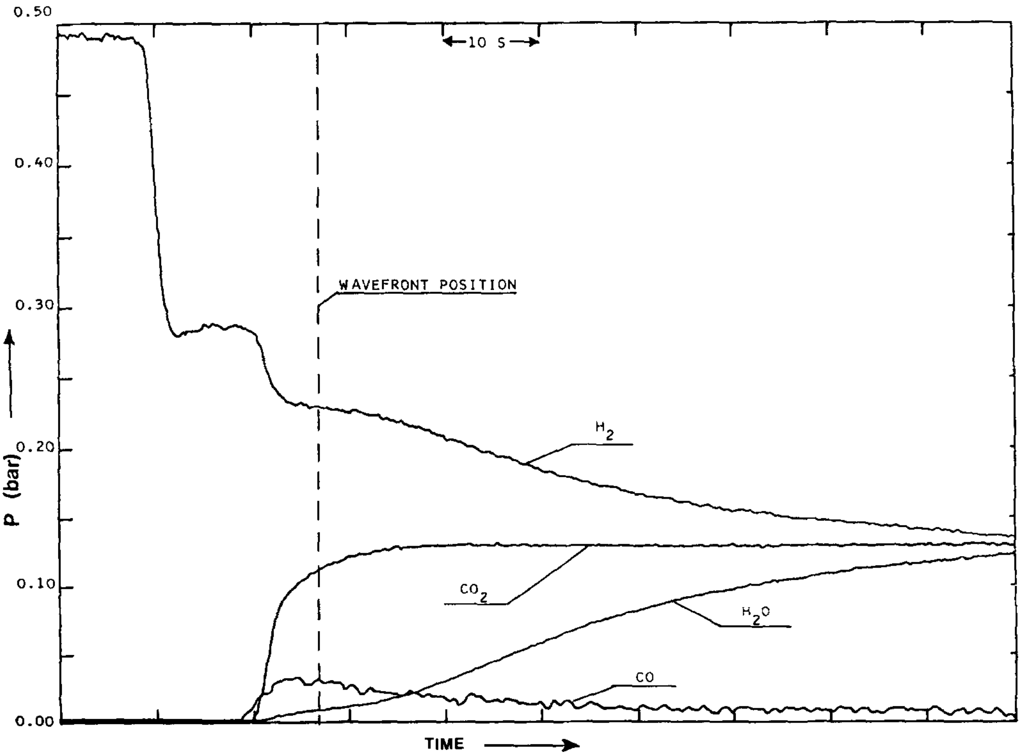

FIG. 1. Concentration transient responses from a similar investigation (*11*) in order to demonstrate the application of wavefront analysis.

converted to H_2 and CO to CO_2 without any significant capacitive effects on the catalyst.

However, even for this extreme situation of highly reduced catalyst at high temperature, the observed time relaxations are slow enough so that despite the (short range) relevant chromatographic effects, the measured amplitudes represent a more or less exact measure of the initial rates of the shift reaction and of the reoxidation process. The latter is manifested in Fig. 1 as overproduction of H_2.

In this investigation, the time relaxations correspond to thermal and surface effects. The observed H_2 and H_2O transients correspond mainly to the reoxidation of the catalyst by the reaction medium and the indicated time gradient could be correlated by Eq. (2). We are confined here to the analysis by means of Eq. (1) of space-relaxation data which correspond to the initial oxygen activity and initial temperature. Thus, the kinetics to be obtained in this paper correspond to the equilibrium between the oxygen distribution on the catalyst surface and the ambient gas mixture, as this has been established during the pretreatment period.

Fitting of the Space-Relaxation Data

The measured amplitudes of H_2 and CO_2 at a given ψ *level* have been fitted to a series of kinetic expressions by means of the least-squares Marquardt routine (*12*). In view of the fact that in this investigation the amplitudes of H_2 and CO_2 differ only slightly, i.e., $p_{H_2} \approx p_{CO_2}$, we have tried at first to fit the data to a *single-path reaction* model.

Table 2 contains the corresponding kinetic expressions.

In agreement with the results of the qualitative analysis, we considered a practically common and quasistationary conversion for H_2 and CO_2. This means that for the amplitudes of H_2 and CO_2 in this kind of dynamic experiment we assumed that the kinetic expressions of Table 2 are the rate controlling ones. The results of the fitting are summarized as follows.

(*a*) *Single-site Langmuir–Hinshelwood kinetics*. The separate fitting of the H_2 or CO_2 data has failed, because the obtained parameters are of the order of magnitude of 10^7.

(*b*) *Stationary redox kinetics*. The fitting was successful but the sum $k_{-1} + k_{-2}$ was significantly negative.

Thereafter, a *three-path reaction* model has been used, as shown in Table 3, which accounts besides the shift reaction also for the reoxidation process between the catalyst surface and the reaction medium. This represents practically an enlargement of the models in Table 2 in the sense that for the CO_2 and H_2 production additional rate terms have been considered, corresponding to nonstationary redox steps. The reduction and oxidation steps, as written in Table 3, are certainly relevant for the conversion

TABLE 2

Single-Path Reaction Models

(a) Single-site Langmuir–Hinshelwood mechanism

$$r_{LH} = \frac{k(p_{CO}p_{H_2O} - p_{H_2}p_{CO_2}/K_p)}{1 + K_1 p_{H_2O} + K_2 p_{CO_2}}$$

(b) Redox mechanism

$$r_{RD} = \frac{k_1 k_2 (p_{CO}p_{H_2O} - p_{H_2}p_{CO_2}/K_p)}{k_1 p_{H_2O} + k_2 p_{CO} + (k_{-1} + k_{-2}) p_{CO_2}}$$

with $p_{H_2} \approx p_{CO_2}$, and therefore only the sum $k_{-1} + k_{-2}$ of the reverse shift reaction parameters, k_{-1} and k_{-2}, can be estimated as a single parameter.

TABLE 3

Three-Path Reaction Models (Preliminary Fitting)

Nonstationary redox reaction

$$CO + (O) \xrightarrow{k_3} CO_2 + (\ \ ),\ \text{i.e., reduction of the catalyst}$$

$$H_2O + (\ \ ) \xrightarrow{k_4} H_2 + (O),\ \text{i.e., oxidation of the catalyst}$$

combined for the shift conversion with:

(a) single-site Langmuir–Hinshelwood mechanism

$$r_{CO_2} = r_{LH} + k_3 p_{CO}\theta_O = r_{LH} + k_3' p_{CO}, \qquad k_3' = k_3\theta_O,$$

$$r_{H_2} = r_{LH} + k_4 p_{H_2O}\theta_{(\ )} = r_{LH} + k_4' p_{H_2O}, \qquad k_4' = k_4\theta_{(\ )},$$

where r_{LH} is the kinetic expression (a) from Table 2, and $\theta_O, \theta_{(\ )}$ are the activities of the oxidizing and reducing surface sites corresponding to the pretreatment of the catalyst, and therefore constant for the analysis of space-relaxation data at constant pretreatment level

(b) redox mechanism

$$r_{CO_2} = r_{RD}' + k_3' p_{CO}$$

$$r_{H_2} = r_{RD}' + k_4' p_{H_2O}$$

where k_3', k_4' are defined as above and r_{RD} is the kinetic expression (b) in Table 2 without the "negative" parameter $k_{-1} + k_{-2}$

$$r_{RD}' = \frac{k_2(p_{CO}p_{H_2O} - p_{H_2}p_{CO}/K_p)}{p_{H_2O} + (k_2/k_1)p_{CO}}$$

at the beginning of the relaxation process (i.e., at the neighborhood of the wavefront), because the catalyst is either further reduced by CO which is here a stronger reducing agent than H_2, or reoxidized by H_2O which is here a stronger oxidizing agent than CO_2, in good agreement with our experimental observations.

The results of the fitting to this three-path model can be summarized as follows:

(*a*) *Nonstationary redox with single-site Langmuir–Hinshelwood mechanism.* The kinetic constants k, K_1, K_2 of the LH expression are here also of the order of magnitude of 10^7 for fitting of both CO_2 and H_2 data; the constants k_3' and K_4' are of the order of magnitude of 10^0. The LH-model seemed therefore nonrealistic to us and has been rejected, because, obviously, the denominator has to be much larger than 1, in order to fit the data to the model, i.e., the LH model has a lack of fit.

(*b*) *Nonstationary redox with a stationary redox mechanism for the shift conversion.* The results of the fitting are contained in Table 4. It is characteristic that the stationary model parameters k_2 and k_2/k_1 are different for the CO_2 and the H_2 fitting, suggesting a lack of fit, too. Furthermore, the parameter k_2/k_1 in the CO_2 fitting is (the $\psi = 5.0$ level excepted) as a rule larger than 1 whereas the same parameter in the H_2 fitting is not significant on the 95% significance level. If one takes into consideration that the term $p_{H_2}p_{CO_2}/K_p$ does not contribute practically (as $K_p \approx 80$), the above result means that the appropriate reaction model in this investigation has to be linear in both CO and H_2O, i.e.,

$$r_{CO_2} = Ap_{CO} + Bp_{H_2O},$$

$$r_{H_2} = A'p_{CO} + B'p_{H_2O}.$$

This linearity of the reaction rate has been established also by a plot of the conversions vs the feed of H_2O and CO depicted in Fig. 2. Therefore, at least in this investigation there exists a simple linear de-

TABLE 4

Results of the Fitting to Model (b) of Table 3[a]

Pretreatment ψ	Fitting of the CO_2 data			Fitting of the H_2 data		
	k_2/k_1	k_2	k_3'	k_2/k_1	k_2	k_4'
0.20	16.349	8.730	0.688	0.065	0.993	0.505
	±2.289	±0.928	±0.110	±0.178	±0.153	±0.094
0.53	16.005	10.422	0.525	0.023	0.813	0.630
	±3.608	±1.901	±0.216	±0.289	±0.230	±0.161
1.00	7.987	4.621	0.561	0.038	0.976	0.340
	±1.471	±0.613	±0.098	±0.080	±0.203	±0.098
2.00	12.045	4.205	0.649	0.448	1.247	0.333
	±3.387	±1.104	±0.205	±0.816	±0.601	±0.247
5.00	2.000	2.030	0.333	0.735	1.583	0.040
	±0.734	±0.398	±0.149	±0.191	±0.127	±0.032
10.00	9.838	2.979	0.674	0.014	0.762	0.168
	±2.062	±0.461	±0.077	±0.057	±0.091	±0.040

[a] ψ = 0.10 is not fitted here.

pendence of the rates on p_{CO} and p_{H_2O}. However, if one takes into consideration the results of the qualitative analysis, that the shift conversion proceeds by the participation of adsorption/desorption intermediates, it seems plausible that the established linearity comes about because certain denominators of hyperbolic rate expressions

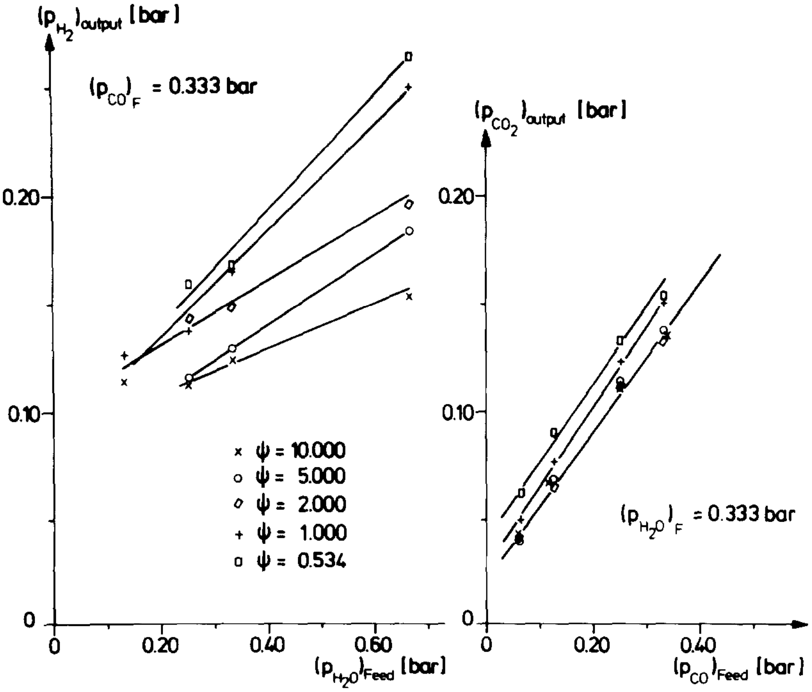

FIG. 2. Linear dependence of conversion on the wavefront on the feed concentrations at different pretreatment levels.

are not significant (i.e., the corresponding capacitances are saturated under the experimental conditions). We suggest therefore the following reaction scheme to account for the space-relaxation data:

(i) formal Eley–Rideal mechanism, CO-adsorbed

$$H_2O + (CO)^* \xrightarrow{k_1} H_2 + CO_2$$

(ii) formal Eley–Rideal mechanism, H_2O-adsorbed

$$CO + (H_2O)^* \xrightarrow{k_2} H_2 + CO_2$$

(iii) redox mechanism

$$\text{(a)}\quad CO + (O) \xrightarrow{k_3} CO_2 + (\ )$$

$$\text{(b)}\quad H_2O + (\ ) \xrightarrow{k_4} H_2 + (O)$$

It is an open question whether in reactions (i) and (ii) the H_2O and CO come from the gas phase or from loose (linear) physisorbed H_2O and CO.

Fitting to the Stationary Formal Eley–Rideal and Nonstationary Redox Mechanism

The space-relaxation data of H_2 and CO_2 have been fitted simultaneously to the linear reaction model stated in Table 5. The simultaneous fitting is possible because the H_2 and CO_2 conversions at the wavefront differ generally one from the other. As the measured conversions correspond to integral data, the following linear matrix differential equation should be solved:

TABLE 5

Formal Eley–Rideal Mechanisms Relevant for the Shift Conversion

(i) $H_2O + (CO)^* \xrightarrow{k_1} H_2 + CO_2$,

where $(CO)^*$ is CO chemisorbed

(ii) $CO + (H_2O)^* \xrightarrow{k_2} H_2 + CO_2$,

where $(H_2O)^*$ is H_2O chemisorbed

The reverse reaction has been neglected, as here $K_p \sim 10^2$.

(iii) Redox mechanism regulating the surface oxygen activity

(a) $CO + (O) \xrightarrow{k_3} CO_2 + (\ )$,

(b) $H_2O + (\ ) \xrightarrow{k_4} H_2 + (O)$,

where (O) is reducible surface oxygen site, ( ) is oxidizable surface site; $(CO)^*$ and $(H_2O)^*$ are in equilibrium with the gas phase, i.e.,

$$\theta_{CO} = \theta_{CO}(T, p_{CO}), \quad \theta_{H_2O} = \theta_{H_2O}(T, p_{H_2O})$$

In this investigation, the adsorption capacity is saturated, i.e.,

$$\theta_{CO} = (\theta_{CO})_{max}, \quad \theta_{H_2O} = (\theta_{H_2O})_{max}$$

Therefore

$$r_i = k_1 p_{H_2O}(\theta_{CO})_{max}$$
$$r_{ii} = k_2 p_{CO}(\theta_{H_2O})_{max}$$

and

$$r_{CO_2} = r_i + r_{ii} + k_3 p_{CO}\theta_{(O)}$$
$$r_{H_2} = r_i + r_{ii} + k_4 p_{H_2O}\theta_{(\ )}$$

$$\frac{d}{dt}\begin{bmatrix} p_{CO} \\ p_{H_2O} \end{bmatrix}_{\alpha_0} = -\begin{pmatrix} k'_2 + k'_3 & k'_1 \\ k'_2 & k'_1 + k'_4 \end{pmatrix}\begin{bmatrix} p_{CO} \\ p_{H_2O} \end{bmatrix}_{\alpha_0}, \qquad (4)$$

which describes the conversion along the propagation line of the wavefront α_0. Whether the parameters k'_3, k'_4 are statistically significant or not is a question which does not influence the nonsingular character of the matrix in Eq. (4).

The solution of Eq. (4) is easily obtained analytically in dependence on eigenfunctions $\exp(m_1\tau_0)$ and $\exp(m_2\tau_0)$, with τ_0 the mean residence time of the disturbance in the catalyst bed. The eigenvalues m_1, m_2 are the solutions of the quadratic equation

$$(k'_2 + k'_3 - m)(k'_1 + k'_4 - m) - k'_1 k'_2 = 0. \quad (5)$$

The results of the fitting can be seen in Table 6, where

$k'_1 = k_1(\theta_{CO})_{max} \approx \text{const}$, because adsorption capacity is saturated,

$k'_2 = k_2(\theta_{H_2O})_{max} \approx \text{const}$, because adsorption capacity is saturated,

$k'_3 = k_3\theta_O \approx \text{const}$, because (O), ( ) correspond to the pretreatment,

$k'_4 = k_4\theta_{(\ )} \approx \text{const}$, because (O), ( ) correspond to the pretreatment.

The eigenfunctions represent a measure of the overall shift activity, which means that the eigenfunction has to be significantly different from 1 in order to contribute to the overall conversion. The eigenvalues $m_{1,2}$ are correlated in this sense with the time constants for the overall rate of the space relaxation as:

$$\tau_{R_{1,2}} = -1/m_{1,2}. \quad (6)$$

DISCUSSION

From the results of the fitting in Table 6 one sees that the redox parameters k'_3, k'_4 are statistically (on the 95% significance level) nonsignificant. The Eley–Rideal parameters k'_1, k'_2 show a rather monotonous dependence on log ψ (as depicted in Fig. 3). The eigenvalues m_1, m_2 of the linear system depend practically linearly on log ψ.

As one can see, for the space relaxation only the eigenfunction $\exp(m_2\tau_0)$ is relevant here. Therefore, only m_2 is dominant and shows a steep decrease with increasing log ψ. The significant decrease in the overall activity by increasing ψ is well in agreement with the experimental observations.

Thereafter one can summarize the above results by saying that the overall activity is expressed by the fact that the eigenvalue m_2 decreases linearly with log ψ. This suggests that the overall reaction kinetics has a logarithmic dependence on the equilibrium relation p_{H_2O}/p_{H_2}, or in other words the oxygen chemisorption follows a logarithmic dependence on the equilibrium relation p_{H_2O}/p_{H_2},

TABLE 6

Results of the Fitting of the Space-Relaxation Data to the Three-Path Reaction Model Consisting of Two Formal Eley–Rideal Mechanisms and One Redox Mechanism for 230°C

ψ	k'_1	k'_2	k'_3	k'_4	m_1	m_2	$\exp(m_1\tau_0)$	$\exp(m_2\tau_0)$
0.10	0.439	1.034	−0.078	−0.018	−0.094	−1.4365	0.995	0.454
	±0.052	±0.076	±0.087	±0.054				
0.20	0.355	0.962	−0.092	0.064	−0.063	−1.294	0.966	0.491
	±0.050	±0.081	±0.095	±0.054				
0.534	0.492	0.804	−0.097	0.069	−0.069	−1.327	0.963	0.482
	±0.097	±0.165	±0.188	±0.109				
1.00	0.375	0.780	−0.081	0.046	−0.061	−1.158	0.967	0.529
	±0.073	±0.105	±0.126	±0.082				
2.00	0.254	0.817	−0.071	0.044	−0.087	−1.061	0.953	0.558
	±0.079	±0.133	±0.166	±0.090				
5.00	0.271	0.724	0.020	−0.036	−0.054	−1.028	0.971	0.568
	±0.078	±0.137	±0.175	±0.089				
10.00	0.194	0.706	0.022	−0.008	−0.032	−0.925	0.983	0.601
	±0.032	±0.049	±0.064	±0.036				

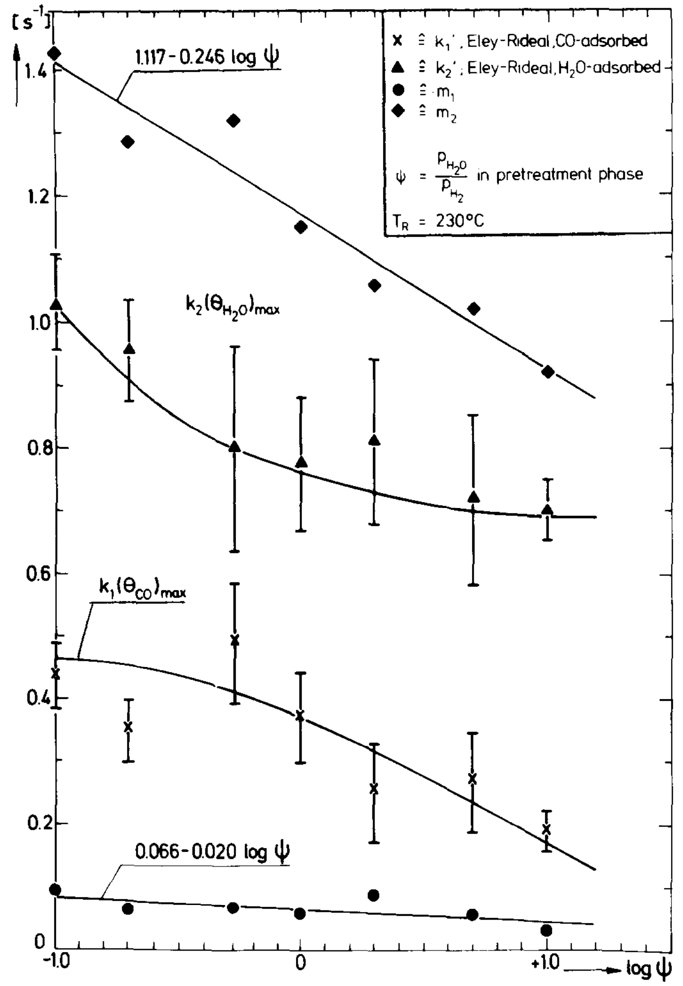

FIG. 3. Dependence of the effective Eley–Rideal kinetic parameters k_1', k_2' and of the eigenvalues m_1, m_2 for the space relaxation on log ψ.

a conclusion which seems to be in agreement with early results by Temkin (*6*). Furthermore, the weight of both mechanisms in the space relaxation is different by changing the oxygen activity. The logarithmic dependence suggests that the redox reaction follows an Elovich-type kinetics.

CONCLUDING REMARKS

The investigations reported here refer to the dependence of the reaction kinetics on the oxygen activity of a CuO/ZnO catalyst. The wavefront analysis is an adequate technique for investigations of this kind, because the space relaxation depends on the thermodynamics and the time relaxation on the kinetics of oxygen activity. The dependence of reaction kinetics on the oxygen chemisorption as established by the equilibrium of the reaction

$$H_2O + (\ ) \rightleftarrows H_2 + (O)$$

has been mainly studied here. The question what is the dependence of the kinetics from the pretreatment until equilibrium for a mixture of CO_2/CO can be easily answered, because the equilibrium ratio $\zeta = p_{CO_2}/p_{CO}$ is coupled with ψ by the thermodynamic equilibrium relation

$$\psi/\zeta = 1/K_p.$$

Since K_p, the equilibrium constant of the shift reaction, in the interesting temperature interval is of the magnitude of 10^2, one has to change ζ in a 100-fold lower interval in order to obtain the same variations in m_2 as with ψ. This makes clear the experimental difficulties with a ζ variation.

At the steady state when catalyst and gas phase are in equilibrium, one has to expect that in any catalytic fixed-bed reactor, an activity profile will be formed, i.e., the overall rate activity of the catalyst is not a unique one, but is a function of the position.

We would like to point out that the three-path kinetic reaction scheme reported here, consisting of the formal Eley–Rideal mechanism and the redox mechanism, seems to be justified by independent dynamic experiments (*6*). Investigations of this type have been performed at higher temperatures (*11*) and they confirmed the validity of the above considerations, too. Furthermore, we assume that the established Elovich dependence on the redox reaction rate, i.e., with a linear dependence of activation energy on oxygen activity, must correspond to a two-dimensional oxide phase on the catalyst surface. The above mentioned investigations (*11*) and investigations on the reduction/oxidation kinetics by H_2/H_2O suggest for the activation energy a most complex dependence, i.e., a quadratic one, rather than the linear one of the Elovich kinetics (*6*), probably because a three-dimensional oxide phase has been built up.

ACKNOWLEDGMENT

It is noted with thanks that reviewers' comments have contributed to a better presentation of this paper.

REFERENCES

1. Wagner, C., *in* "Advances in Catalysis" (D. D. Eley, H. Pines, and P. B. Weisz, Eds.), Vol. 21, p. 323. Academic Press, New York, 1970.
2. Temkin, M. I., *Kinet. Catal. USSR* **17,** 945 (1976).
3. Boreskov, G. K., *Kinet. Catal. USSR* **21,** 1 (1980).
4. Fiolitakis, E., Hoffman, U., and Hofmann, H., *Chem. Eng. Sci.* **34,** 677 (1979).
5. Fiolitakis, E., and Hofmann, H., *Catal. Rev. Sci. Eng.* **24,** 113 (1982).
6. Fiolitakis, E., "Wellenfrontanalyse, eine Übergangstechnik und eine spezifische Analyse von Übergangsantworten zur Untersuchung heterogen katalytischer Systeme." Habilitationsschrift, Erlangen, 1981.
7. Fiolitakis, E., "Some Aspects on the Entropy Change in Onsager's Sense for Irreversible Chemical Processes." To be published.
8. Fiolitakis, E., Hoffmann, U., and Hofmann, H., *Chem. Eng. Sci.* **35,** 1021 (1980).
9. Fiolitakis, E., and Hofmann, H., *Chem. Ing. Tech.* **51,** 800 (1979).
10. Fiolitakis, E., and Hofmann, H., ACS Symp. Ser. 178, p. 277 (1982).
11. Kaleńczuk, R. J., Fiolitakis, E., and Hofmann, H., *Chem. Ing. Tech.* **52,** 966–968 (1980).
12. Marquardt, D. W., Share Program Library, SDA No. 3094.